Pergamon

PII S0016-7037(97)00384-0

Origin of geochemical heterogeneity in the mantle peridotites from the Bay of Islands ophiolite, Newfoundland, Canada: Ion probe study of clinopyroxenes

V. G. Batanova,[1] G. Suhr,[2,]* and A. V. Sobolev[1]

[1]Vernadsky Institute of Geochemistry, Russian Academy of Sciences, Moscow, 117975, Russia
[2]Institute of Mineralogy and Petrology, University of Köln, 50674 Köln, Germany

Abstract—Representative samples from a 6 km thick ophiolitic mantle section were selected for ion probe analysis of clinopyroxene (cpx). The purpose was to evaluate the trace element heterogeneity occurring on a kilometer-scale in the geologically well constrained uppermost mantle beneath the ancient Bay of Islands ophiolite spreading center. The range of REE patterns in the mantle section can be explained by 7–20% near-fractional melting of a weakly depleted mantle source followed by varying degrees of trace element chromatographic exchange between an interstitial liquid and the refractory residue and/or precipitation of phases from the interstitial liquid. Peridotites from the basal mantle section are the least depleted ones. They require little to no overprint by melt circulation and can be modeled as residues of fractional melting with a low (0.1%) residual porosity. Their presence in the mantle section is possibly related to ductile accretion of less depleted peridotite during ophiolite obduction. Peridotites from the central, but mainly uppermost mantle section require stronger interaction with percolating melts. Uppermost peridotites also show the highest spatial variability in the degree of depletion. A preferred, but nonunique model for their formation is refertilization of initially more refractory residues due to cpx ± plagioclase addition from liquids depleted relative to N-MORB. Such depleted liquids are also inferred from wehrlitic rocks occurring in the crust-mantle transition zone. They may have originated as melts emerging from mantle columns or mixtures of such melts, i.e., melts whose compositions were affected by reaction with a large volume of mantle rocks. *Copyright © 1998 Elsevier Science Ltd*

1. INTRODUCTION

Decompression melting beneath mid-ocean ridges leads to a chemically stratified residual mantle column (Langmuir et al., 1992) due to progressive extraction of basaltic components from lherzolite (McKenzie, 1984; Nicolas, 1986). As a result, residual mantle directly underlying the oceanic crust should represent the most depleted mantle; its degree of depletion being a first order function of the mantle potential temperature (McKenzie and Bickle, 1988). Further factors influencing the extent of melting reached at a mid-ocean ridge are the mode of melting (batch vs. fractional; Langmuir et al., 1992; Hess, 1992), source heterogeneity (Dick and Natland, 1995), and the intensity of conductive cooling at shallow mantle depth (Forsyth, 1993). Rare earth element (REE) abundances in clinopyroxene (cpx) have proven to be an efficient way to evaluate the degree of chemical depletion in peridotite (Johnson et al., 1990; Johnson and Dick, 1992; Hauri and Hart, 1994; Rampone et al., 1996; Ozawa and Shimizu, 1995).

In some ophiolites, a coherent crust-mantle boundary is preserved, and the exposed uppermost mantle should be the most depleted residual rock in the mantle column. In addition to partial melting, the uppermost peridotites of the oceanic mantle are also traversed by melts segregated at greater depth. Whether this migration of melts occurred in dykes, by large scale migration within the grain boundary network or by some kind of focused porous flow or by a combination of all above is a matter of debate (Bodinier et al., 1996; van der Wal and

Bodinier, 1996; Godard et al., 1995; Kelemen et al., 1995a,b, 1997; Sleep, 1988). The chemical effect of the interaction between migrating melts and a peridotite matrix has been modeled by chromatographic processes (McKenzie, 1984; Navon and Stolper 1987; Bodinier et al., 1990; Vasseur et al., 1991). In this model, the migration of even small amounts of melt through peridotite can be traced as changes in the concentration of highly incompatible elements in the solid. Less incompatible elements (with respect to the peridotite mineralogy), on the other hand, are more robust against changes during melt migration. Abundances of REE (which range from highly to moderately incompatible under upper mantle conditions) are useful to track melt migration processes (e.g., Hauri and Hart, 1994). Specifically, the enrichment in LREE, seen in bulk rock and cpx analyses of many mantle peridotites (McDonough and Frey, 1989) has been attributed to the migration of melts which are in equilibrium with a relatively fertile peridotite in contrast to the depleted peridotite they migrated through.

The purpose of this study is to evaluate both the degree of depletion and the degree of melt-peridotite reaction in an ophiolitic mantle section using REE analysis of cpx in harzburgite and lherzolite.

2. PREVIOUS WORK

2.1 Geologic Background

The Bay of Islands ophiolite represents 485 my old oceanic lithosphere preserved in a relatively intact nature on the west coast of the island of Newfoundland (Fig. 1, inset; Dunning and Krogh, 1984; Williams, 1979). While major element (Siroky et al., 1985), REE (Suen et al., 1979; Jenner et al., 1991; Elthon, 1991), and isotopic data (Jacobsen and Wasserburg 1979; Jen-
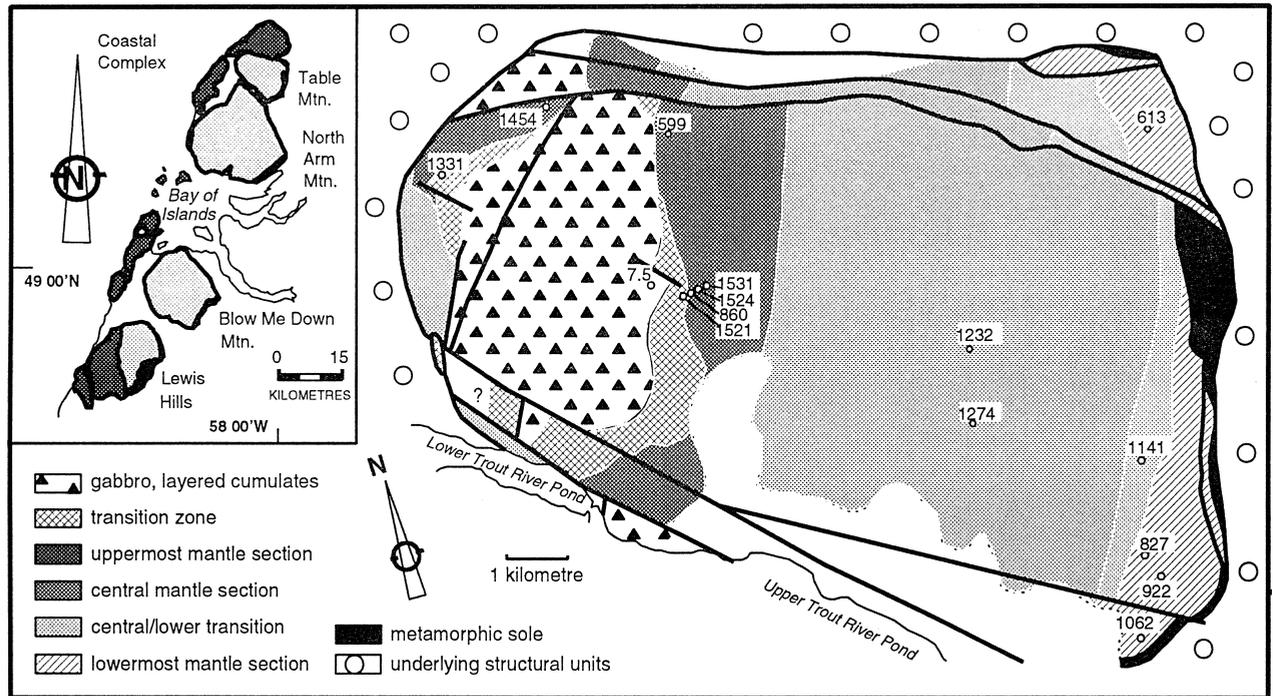
Fig. 1. Schematic geologic map of Table Mountain massif showing studied samples locations and location of massifs within the Bay of Islands Ophiolite (inset).

ner et al., 1991) of the upper crustal rocks of the ophiolite are akin to mid-ocean ridge basalt (MORB) (Casey et al., 1985), Ta and Nb abundances in these rocks suggest a formation above a subducted slab (Elthon, 1991; Jenner et al., 1991), e.g., in a back-arc basin. Differences from MORB have also been inferred for dyke rocks and lower crustal cumulates occurring within the Lewis Hills and North Arm Mountain (Elthon et al., 1986; Edwards, 1990; Edwards and Malpas, 1995; Bédard and Hébert, 1996; Varfalvy et al., 1997). Samples for this study are from Table Mountain, the northernmost of four massifs of the Bay of Islands Ophiolite.

The geologic map of the Table Mountain massif is shown in Fig. 1 together with the studied sample locations. The lowermost mantle section (depth 5–6 km below the crust-mantle transition) is characterized by generally coarse grained peridotites which define a steep chemical gradient ranging from lherzolites (samples TM 1062, 922, 613) at the base of the ophiolite with a Cr# ($100Cr/(Cr + Al)$) in spinel of <20 to harzburgites (sample TM 827; Suhr and Robinson, 1994). The lherzolites generally display a high strain overprint acquired during ophiolite detachment.

The central mantle section (depth 2–5 km) is dominated by cpx-poor harzburgites (samples TM 1232, TM 1274). Stretching lineations indicate a strong ridge-parallel flow component. Sample TM 1141 comes from an area rich in dunitic pods and bands typically present at the boundary between the central and lowermost mantle section. The sample is an opx-depleted harzburgite.

The uppermost mantle section (depth 0–2 km), defined by a marked change in the high temperature stretching lineation from oblique to normal to the ridge, was interpreted on the basis of geological, microstructural, and mineral chemical data to contain a significant proportion of trapped melt or

minerals formed from migrating melts (Suhr, 1992, 1993; Suhr and Robinson, 1994). This is seen in the field as cpx-rich harzburgite (sample TM 1454), lherzolite (TM 599), or, in one observed case, several meters of plagioclase lherzolite (sample TM 1524). Locally, cpx-poor harzburgite occurs (sample TM 1531). This uppermost mantle section contains also rare wehrlitic layers (sample TM 860) for which an origin by cumulate processes or as a melt-peridotite reaction product from a harzburgitic precursor could not be conclusively resolved.

Above the opx-bearing mantle rocks, poorly to unlayered dunites, cpx-dunites, wehrlites, and plagioclase-bearing wehrlites occur with a thickness up to 500 m. Sample TM 1521 comes from the immediate harzburgite-dunite transition; plagioclase wehrlite TM 1331 is from within this sequence. Since this entire section is plastically deformed, their origin by cumulate processes or by in situ transformation of mantle rocks (e.g., Nicolas 1989) is difficult to resolve. The rocks are referred to as transition zone rocks (Nicolas and Prinzhofer, 1983). Up-section, a layered ultramafic-mafic sequence follows (sample olivine clinopyroxenite TM 7.5). The major element compositions of selected rocks are published in Suhr and Robinson (1994).

2.2. Mineral Chemistry

Mineral chemical data have been collected regionally over the mantle peridotites (Suhr and Robinson, 1994). A partial melting trend was defined in a plot of the Cr# in spinel vs. the Mg# ($100Mg/(Mg + Fe)$) in olivine. It was distinguished from a melt impregnation trend. The partial melting trend is defined by samples from the central and lowermost peridotites, the latter ones being least depleted. Their Cr#'s are as low as 10.

Table 1. Clinopyroxene compositions

Sample	Rock	SiO$_2$	TiO$_2$	Al$_2$O$_3$	Cr$_2$O$_3$	FeO	MgO	MnO	CaO	Na$_2$O	Ti	Y	La	Ce	Nd	Sm	Eu	Dy	Er	Yb
TM 273[A]													0,047	0,08	0,088	0,11	0,065	1,35	0,78	0,78
TM 273[B]													0,030	0,074	0,087	0,097	0,062	1,84	0,95	0,68
tv5[C]											710	7,2	0,007	0,011	0,05	0,10	0,08	1,20	0,64	0,71
tv5[D]	Lhz	52,06	0,16	4,48	1,08	2,30	16,74	0,08	23,64	0,20	702	6,3	0,009	0,010	0,04	0,12	0,06	0,97	0,63	0,71
TM 1062	Lhz	50,86	0,22	6,87	1,14	3,50	17,48	0,13	19,01	0,82	1186	12,8	0,006	0,03	0,45	0,58	0,25	2,04	1,31	1,35
TM 613	Lhz	52,40	0,07	4,31	1,11	2,55	17,74	0,08	21,40	0,23	358	5,9	0,003	0,010	0,03	0,09	0,07	0,84	0,70	0,72
TM 922	Lhz	51,04	0,10	5,43	1,08	3,13	16,89	0,12	21,09	0,29	549	7,8	0,003	0,005	0,06	0,16	0,09	1,23	0,86	0,88
TM 827	CHz	52,26	0,06	3,96	1,14	3,03	18,79	0,09	20,90	0,13	361	4,7	0,003	0,01	0,03	0,07	0,04	0,65	0,54	0,58
TM 1141	Hz	54,54	0,03	2,22	1,15	1,96	17,61	0,08	22,22	0,47	159	2,3	0,16	0,38	0,22	0,09	0,03	0,34	0,30	0,30
TM 1274	Hz	54,09	0,01	2,37	0,84	1,94	17,63	0,05	23,58	0,01	116	1,3	0,007	0,02	0,015	0,015	0,006	0,12	0,18	0,28
TM 1232	Hz	53,91	0,01	2,27	0,70	1,84	18,44	0,06	22,24	0,06	106	1,0	0,01	0,03	0,02	0,02	0,007	0,12	0,11	0,17
TM 599	Lhz	52,09	0,05	4,22	1,10	2,79	17,26	0,08	21,75	0,22	273	4,1	0,04	0,11	0,13	0,09	0,04	0,58	0,51	0,55
TM 1454	CHz	52,32	0,08	3,82	1,01	2,65	17,85	0,07	21,51	0,25	383	4,4	0,02	0,05	0,14	0,13	0,05	0,63	0,49	0,53
TM 1531	CHz	53,20	0,05	2,08	0,85	2,62	17,48	0,10	22,91	0,03	261	2,2	0,017	0,07	0,06	0,07	0,035	0,38	0,23	0,21
TM 860	Wh	53,23	0,11	2,29	0,79	3,27	17,54	0,11	22,39	0,19	568	3,4	0,08	0,29	0,42	0,26	0,12	0,62	0,36	0,35
TM 1524	Pl Lhz	53,23	0,11	2,29	0,79	3,27	17,54	0,11	22,39	0,19	1983	20,8	0,05	0,30	1,07	0,99	0,33	3,43	2,27	1,97
TM 1521	Opx Wh	53,72	0,11	1,93	0,90	3,00	17,63	0,10	22,81	0,17	596	4,4	0,04	0,15	0,37	0,32	0,13	0,88	0,48	0,52
TM 1331	Pl Wh	52,80	0,16	4,11	1,24	2,47	16,38	0,08	22,82	0,52	1053	4,9	0,01	0,07	0,29	0,28	0,16	0,84	0,55	0,64
TM 7.5	Ol Pxt	53,68	0,56	3,44	0,75	6,32	16,52	0,16	20,51	0,33	4021	19,7	0,25	1,32	2,63	1,56	0,73	3,73	2,25	2,14

Concentration of oxides in wt.%, concentration of trace elements in parts per million by weight.
A and B - cpx of sample TM 273 analysed in WHOI and in IMAN, Yaroslavl respectively
C and D- cpx sample tv5, analysed in CSCC, Pavia and in IMAN, Yaroslavl, respectively
Rock names: Lhz - spinel lherzolite, CHz - cpx-bearing harzburgite, Hz - harzburgite, Wh - wehrlite, Pl Lhz - plagioclase lherzolite, Opx Wh - opx-bearing wehrlite, Pl Wh - plagioclase wehrlite, Ol Pxt - olivine clinopyroxenite
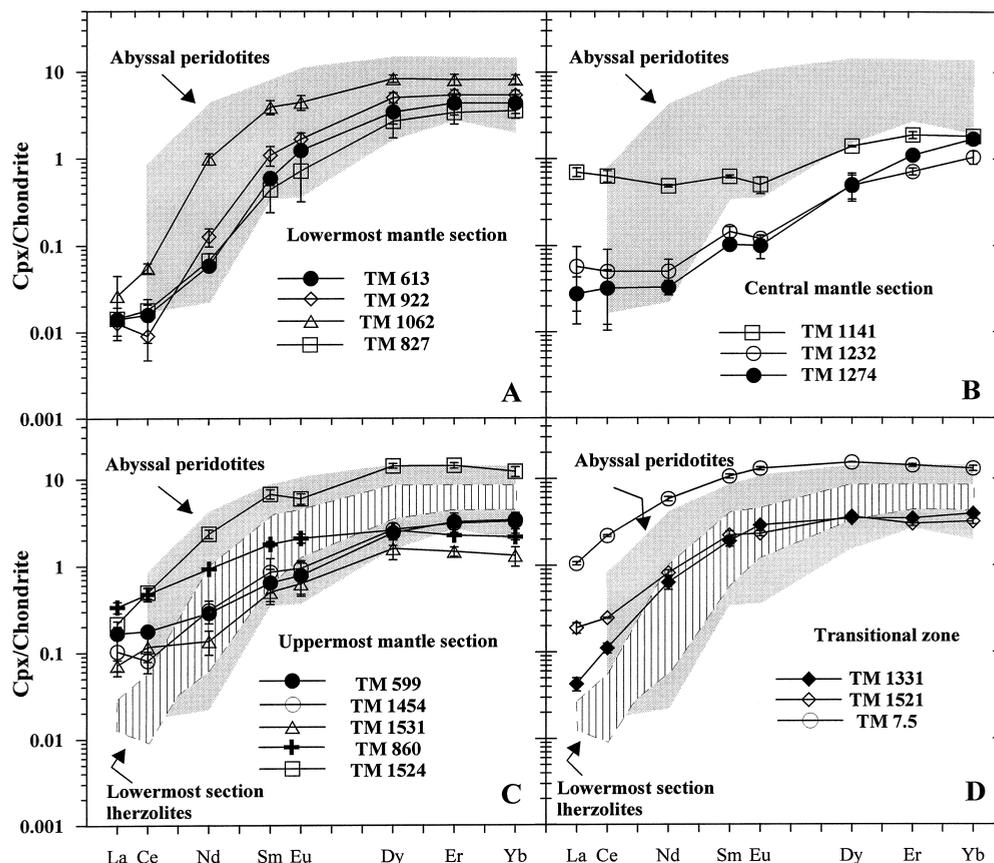
Fig. 2. Rare Earth element data for clinopyroxenes (cpx) from Table Mountain massif, relative to C1 chondrite values (Anders and Grevesse, 1989). (a) Cpx of lowermost mantle section peridotites: TM 1062, TM 922, TM 613: spinel lherzolite; TM 827: cpx-bearing harzburgite. (b) Cpx of central mantle section harzburgites. (c) Cpx of uppermost mantle section peridotites: TM 599: spinel lherzolite, TM 1454: cpx-bearing harzburgite; TM 1531: cpx-poor harzburgite; TM 860: wehrlite; TM 1524: plagioclase lherzolite. (d) Cpx of transition zone rocks: TM 1331: plagioclase wehrlite; TM 1521: opx-bearing wehrlite; TM 7.5: olivine clinopyroxenite. Shaded field of abyssal peridotites after Johnson et al. (1990) and Johnson and Dick (1992). Error bar corresponds to 1σ.

The melt impregnation vector is most pronounced in the uppermost peridotites and is best seen as an increase of TiO_2 in spinel and a decrease of the Mg# in olivine for a given Cr# in spinel. Dunite pods and associated harzburgites from the dunite-enriched region above the lowermost peridotites have spinels with very high Cr# up to 85.

3. ANALYTICAL METHOD

REE analyses of cpx from the Table Mountain peridotites were obtained by a Cameca IMS 4f ion probe, Institute of Microelectronics (IMAN), Russian Academy of Sciences, Yaroslavl, Russia, using energy filtering techniques (Shimizu and Hart, 1982). All elements were analyzed using the ratio of their most abundant isotopes to ^{30}Si isotope. Typical run conditions are as following: secondary ion voltage offset −50 eV, energy slit width 50 eV, primary beam current intensity 1–10 nA, primary beam net energy 14.5 keV, primary beam diameter 20–40 μm, primary beam ion O^- (Sobolev and Batanova, 1995). The spectra were accumulated during five cycles with a total of 40–50 min counting time. The accuracy of the measurements estimated from the reproducibility of the standards, Monastery garnet (Roden and Shimizu, 1993) and Kilbourne Hole cpx (Czamanske et al., 1993; Sobolev et al., 1996), is better than 20% relative for most elements. The measurements were performed in polished thin sections. For each thin section, three to five analyses from two to three mineral grains were typically obtained. Point to point trace element abundances in the clinopyroxenes vary less than 10–20% relative, with the exception of some low-level REE measurements approaching the detection limit (where uncertainties may be as high as 40–50% relative). Duplicate analyses of a specific cpx grain analyzed previously at the Woods Hole Oceanographic Institute (WHOI) yielded a good reproducibility (Table 1). Additionally the detection limits for LREE were checked by replicate measurements of highly depleted cpx from Troodos lherzolites (Sobolev and Batanova, 1995) with different secondary ion energy offset. The data obtained at IMAN at −50 eV voltage offset and at CSCC (CNR-Centro di Studio per la Cristallochimica e la Cristallografia, Pavia) at −100 eV offset, 50 eV energy window, show excellent correspondence (see Table 1, sample tv5) suggesting that the actual detection limits (DL) of our method are less than 10 ppb for La and Ce. The detection limits for La and Ce can be estimated by assuming that the entire olivine signal from the studied lherzolites belongs to the background. The measured background and sensitivity values are 0.08 cps and 50 cps/ppm, respectively, for La and 0.17 cps and 40 cps/ppm, respectively, for Ce which yields DL (La) = 1.6 ppb and DL (Ce) = 4.3 ppb. Because cpx grains from the studied samples are chemically homogeneous within quoted errors, we report here average compositions of cpx (Table 1).

4. RESULTS

Concentrations of the REE for the analyzed cpx are given in Table 1 and shown in Fig. 2. Spinel lherzolites and cpx-bearing harzburgites from the lowermost mantle section in TM have strongly fractionated REE patterns (Fig. 2a). Their composition
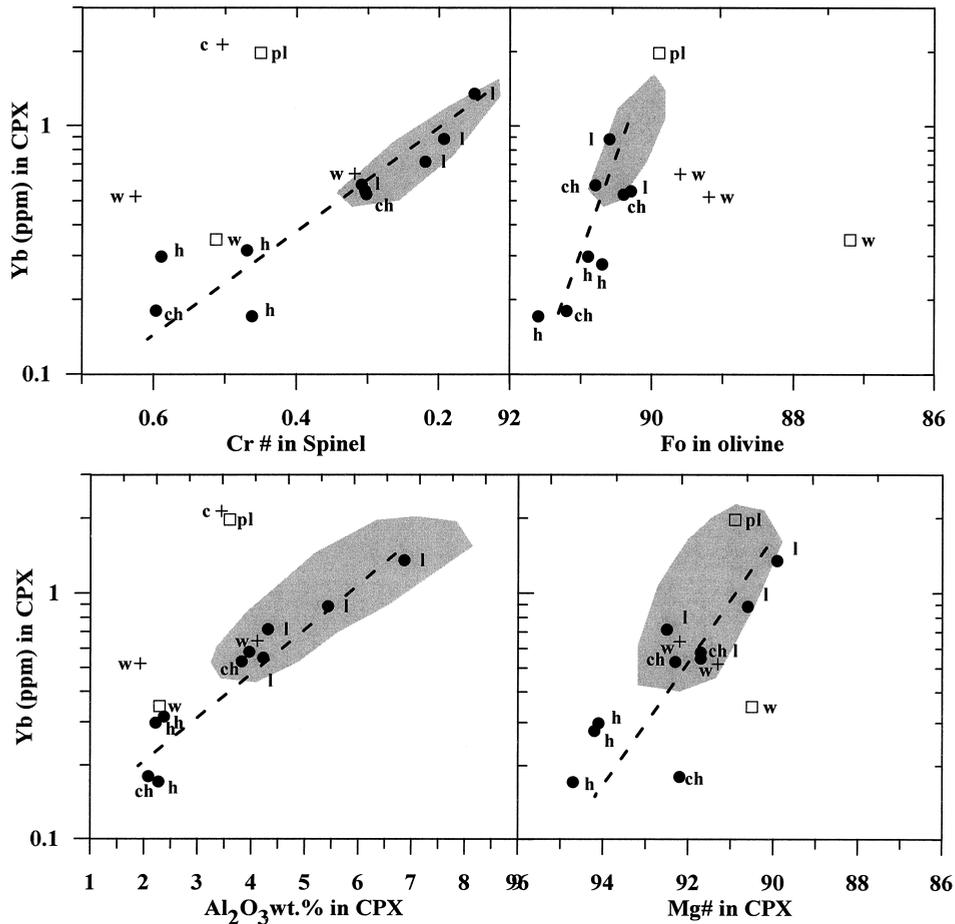
Fig. 3. Correlation between Yb (ppm) in clinopyroxene and mineral chemistry of peridotites from Table Mountain massif. *Filled circles:* residual mantle peridotites; *open square:* wehrlite TM 860, plagioclase lherzolite TM 1524; *cross:* lithologies from the transition zone rocks. *l:* spinel lherzolites, *h:* harzburgites, *ch:* clinopyroxene-bearing harzburgites, *pl:* plagioclase lherzolite, *w:* wehrlite, *c:* olivine clinopyroxenite. *Shaded field:* abyssal peridotite after Johnson et al. (1990), Johnson and Dick (1992), and Dick (1989).

plots within the field of abyssal peridotites (Johnson et al., 1990; Johnson and Dick, 1992).

Clinopyroxenes from the cpx-poor central mantle section (TM 1232, TM 1274) have lower concentrations of the HREEs which are significantly more depleted than the abyssal peridotite range (Fig. 2b). On the other hand, they have higher LREE/HREEs than the cpx from the lowermost mantle section (Fig. 2b). An extreme case is represented by sample TM 1141. Its HREE content is comparable to the other samples from the central mantle section but its LREE and MREE content is strongly enriched, resulting in an overall nearly flat pattern. In addition, the sample is strongly depleted in opx (10% modal opx).

Harzburgites and lherzolites from the uppermost mantle section (Fig. 2c) are characterized by rather low, but flat HREE concentrations and only very moderate LREE depletion compared to the abyssal peridotite range. Notable is the very high HREE content of the plagioclase lherzolite TM 1524.

The REE patterns of the transition zone rocks (Fig. 2d) are overall similar to each other but the absolute abundance of REEs varies considerably between the samples. The wehrlitic cpx (sample TM 860, Fig. 2c) from the uppermost mantle

section shows similar trace element patterns to cpx grains from the transition zone rocks.

The residual mantle rocks display a strong correlation between their mineral chemistry and HREE abundances of cpx. Figure 3 shows the strong negative correlation between Yb content in cpx and the Cr# of spinel, the Mg# of cpx and the Mg# of olivine, and a positive correlation between Yb content in cpx and its Al concentration. The observed trends overlap significantly with those from abyssal peridotites (Fig. 3). The wehrlite layer TM 860, the plagioclase lherzolite TM 1524, and the lithologies from the transitional zone deviate from the trends. They are characterized by a higher Cr# of spinel and a lower forsteritic content of olivine and Mg# of cpx. Plots involving Al-partitioning are influenced by the presence of plagioclase as in TM 1524. Contrary to the HREE, LREE contents in the studied peridotites from the mantle section show neither a correlation with the mineral composition (Fig. 4) nor do they fit into the trend of abyssal peridotites.

The observed correlations between the HREE contents in cpx and major element compositions of the minerals can be explained as a result of variable degrees of partial melting (Johnson et al., 1990; Johnson and Dick, 1992). The lack of
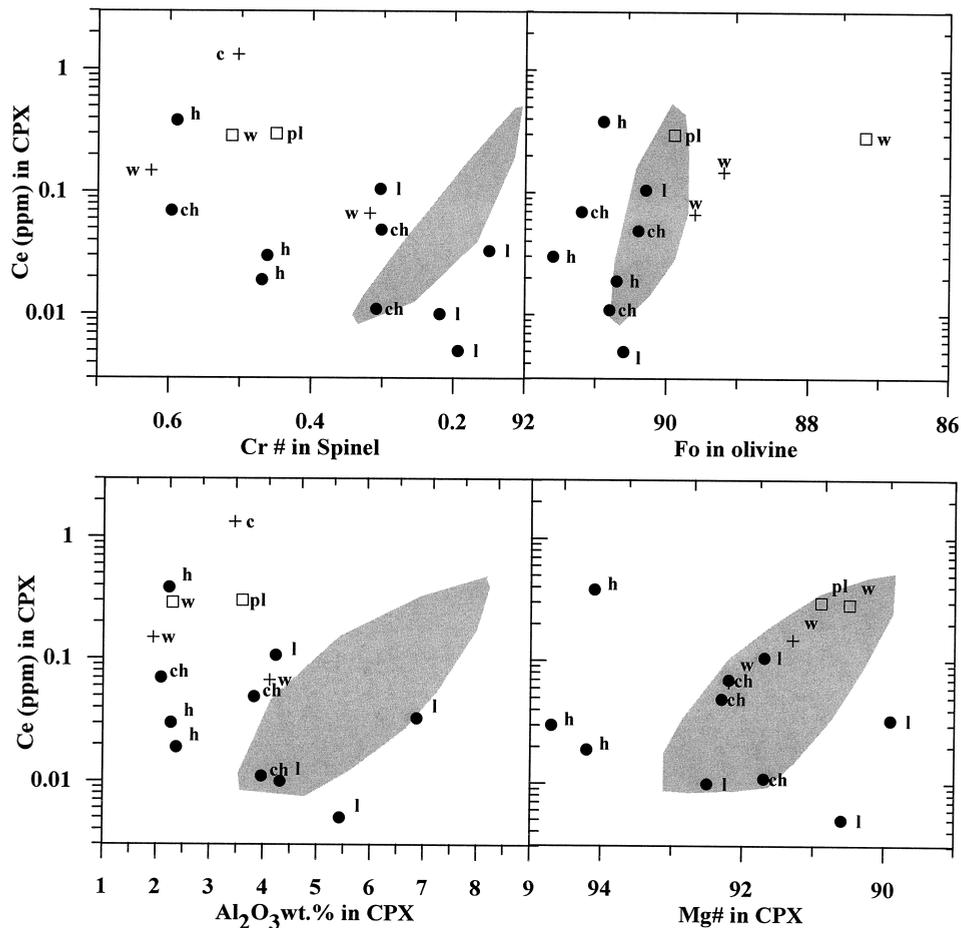
Fig. 4. Correlation between Ce (ppm) in clinopyroxene and mineral chemistry of peridotites from Table Mountain massif. Symbols are as in Fig. 3.

such a correlation for the LREE suggests the operation of another process which, however, did not significantly affect the HREE concentrations. Such a decoupling of HREE and LREE is commonly attributed to reaction of a solid with a relatively enriched melt (chromatographic process, Navon and Stolper, 1987; Bodinier et al., 1990; Vasseur et al., 1991). Thus the observed REE compositions of cpx from mantle peridotites may indicate at least a two stage history: different extents of melting in the mantle column followed by variable extents of incompatible trace element exchange with percolating melts.

5. MODELING

5.1. General Approach

Modeling is started with a partial melting event. This is followed, if required, by a melt percolation event in which melt and solid are in trace element disequilibrium but major element (i.e., modal) equilibrium. A critical melting model (Maaloe 1982) is applied using the analytical solution given in Sobolev and Shimizu (1992). During critical melting, melt extraction occurs after a porosity threshold has been exceeded. Beyond this residual porosity, the melting process is fractional and extraction is continuous. The melting process takes place within the spinel-stability field; it is nonmodal and leads to exhaustion of cpx after 22% partial melting. Initial and pro-

gressive chemical and modal compositions of the mantle source, melting mode, and mineral/melt partition coefficients are given in Table 2. The residual mantle porosity affects the fractionation between elements of different compatibility. The value of 0.1% for this parameter was found to give a best fit for the REE in the studied lowermost spinel lherzolites and was, therefore, used for all samples even though for peridotites from the central and upper mantle section there is no good constraint for the residual porosity during melting. An exception is sample TM 1141 for which a residual porosity of 2% had to be used. The range of 0.1–2% is within the range reported for MOR peridotites (Johnson and Dick, 1992) and MORB (Sobolev and Shimizu, 1992, 1993). In order to define the extent of melting, the HREE concentration of the mantle rocks was used. Implicitly it is therefore assumed that the HREE have not strongly been affected by the following melt percolation event (cf. Hauri and Hart, 1994). This approach is supported when the calculated mode of the residue from the melting model matches that of the sample. Table 3 shows that the correspondence is acceptable except for TM 1141 and TM 1524. These samples are dealt with separately further below.

For modeling the melt-host trace element exchange the code for percolation-controlled metasomatism developed by Bodinier et al. (1990) was used. In this model, trace element exchange between solid and fluid occurs by diffusion over the

Tab. 2. Critical melting model: input parameters and results

Element	Distribution coefficients[a] olivine/liq	opx/liq	cpx/liq	spinel/liq	Source composition DMant[b]	Composition of residual mantle matrix[c] F=7%	F=11%	F=13%	F=14%	F=19%	F=20%	F=20%	column melt from TM 922
La	0.000031	4.40E-05	0.0536	0.0006	0.31	5.936E-05	7.698E-08	1.234E-09	1.17E-10	4.6366E-18	1.9874E-20	4.3425E-06	0.38868
Ce	0.0001	1.40E-04	0.0858	0.0006	0.95	0.0037	4.64E-05	2.967E-06	6.113E-07	4.47E-12	8.2229E-14	4.81E-05	0.3672
Nd	0.00042	5.20E-04	0.1873	0.0006	0.86	0.0637	0.0080	0.0021	0.0010	2.58E-06	3.0589E-07	5.17E-04	0.46233
Sm	0.0011	1.60E-03	0.291	0.0006	0.32	0.0612	0.0163	0.0070	0.0043	9.34E-05	2.3629E-05	8.92E-04	0.5814
Eu	0.00075	6.40E-04	0.35	0.0006	0.13	0.0325	0.0106	0.0051	0.0034	1.20E-04	3.4545E-05	5.68E-04	0.3248
Dy	0.0014	8.40E-03	0.442	0.0015	0.64	0.224	0.096	0.056	0.041	0.004	0.00150062	0.007	2.2352
Er	0.013	1.70E-02	0.44*	0.003	0.4	0.160	0.079	0.051	0.040	0.008	0.00458483	0.012	1.50605
Yb	0.03	0.033	0.43	0.0045	0.43	0.199	0.113	0.081	0.068	0.022	0.01615603	0.028	1.7
α (wt.%)						0.1	0.1	0.1	0.1	0.1	0.1	2	
Phase proportions													
olivine					0.57	0.628	0.665	0.685	0.695	0.751	0.763	0.775	
opx					0.24	0.228	0.220	0.216	0.214	0.202	0.200	0.197	
cpx					0.16	0.118	0.091	0.076	0.069	0.029	0.020	0.011	
spinel					0.03	0.026	0.024	0.023	0.022	0.018	0.018	0.017	

a) crystal/liquid distribution coefficients: olivine and orthopyroxene (opx) after Kennedy et al 1993, clinopyroxene (cpx) after Hart & Dunn, 1993, * Er is ajusted as average between Dy and Yb, spinel from Kelemen et al. (1992)

b) composition of depleted mantle source (in ppm) and phase proportions in it after Johnson et al, 1990

c) compopsition of residual mantle matrix (and phase proportions in it) calculated by critical (continuous) melting model from Sobolev & Shimizu, 1992. F - degree of melting, melting mode: olivine= -0.2, opx= 0.4, cpx=0.72, spinel=0.08,

d) column melt from lower mantle section (conditions for TM 922, TM 613, Tab. 3)

α − amount of critical melt retained in residue

surface of the solid, such that the grain size, as deduced from the samples, is an important input parameter. Transport of components in the melt is by advection with a percolation velocity v. Diffusive transport within the melt along the mantle column is neglected. The solid matrix is considered as having average properties which can be expressed as one bulk distribution coefficient D and a mean grain radius for spherical grains. Since the Bay of Islands ophiolite is characterized by an upper crustal carapace with MORB-like REE patterns, the melt entering at the base of a column is assumed to be average N-MORB (Sun and McDonough, 1989). The critical time tc is the time it takes for the melt to cover the distance from the base of the column of length L to the sample (tc = L/v). For example, for the percolation time t = 2 tc an entire column volume of melt has passed the sample.

This modeling approach is not unique. For example, it could also be attempted to model all rocks as residues of a fixed, high, or low extent of melting followed by subsequent, but variable, nonmodal interaction with percolating melts. Geologic evidence is, therefore, crucial in guiding the modeling approach. The regional survey of the mantle section (Suhr and Robinson, 1994) showed that large scale, smooth variations in the mineral chemistry exist except in the uppermost mantle section (samples TM 1524, TM 599, TM 1454, TM 860, TM 1531) and in

Tab. 3. Percolation model: input parameters and results

Sample	Lowermost mantle section[d] TM 1062	TM 922 TM 613	TM 827	Central mantle section TM 1274 TM 1232	TM 1141	Uppermost mantle section TM 1531	TM 599 TM 1454	TM 1524
column length L (m)	1000	600	600	100	200	10	10	
percol velocity (cm/yr)	5	10	10	10	10	20	20	
t (tc)	1.3	1.05	1.05	1.05	1.3	1.3	2.2	
t (year)	26000	6300	6300	1050	2600	65	110	
residue from % melting	7%	11%	13%	19%	20%	20%	14%	TM 1531
grain size (cm)	0.3	0.3	0.3	0.2	0.1	0.1	0.2	
porosity	0.01	0.01	0.01	0.01	0.01	0.02	0.02	
percolating melt	NMORB	NMORB	NMORB	NMORB	NMORB	NMORB	NMORB	col-melt*
cpx model (%)[a]	11.8	9.1	7.6	2.9	2	2	6.9	1
opx model (%)	22.8	22	21.6	20.2	20	20	21.4	20
cpx mode (%)[b]	9	6.5	4.3	0.9	0.5	0.2[c]	5.4	5.2[c]
opx mode (%)	25	25.1	21.9	14.4	9.7	12.9[c]	18.2	19.3[c]

a) cpx and opx modes from model (see table 2)

b) cpx and opx modes derived from mass balance using CaO data from bulk rock and mineral chemistry (Suhr and Robinson, 1994), and estimated opx/ol proportions from thin sections.

c) by point counting

d) for this section could also be lack of percolation pending on significance attached to LREE

*) 10% trapped column melt (as it emerges from TM 922/TM 613) crystallizes as cpx and plag in equal proportions

Diffusion coefficient in matrix $D=10^{-13}cm^2/s$, geometric parameter α (Bodinier et al., 1990) = 20
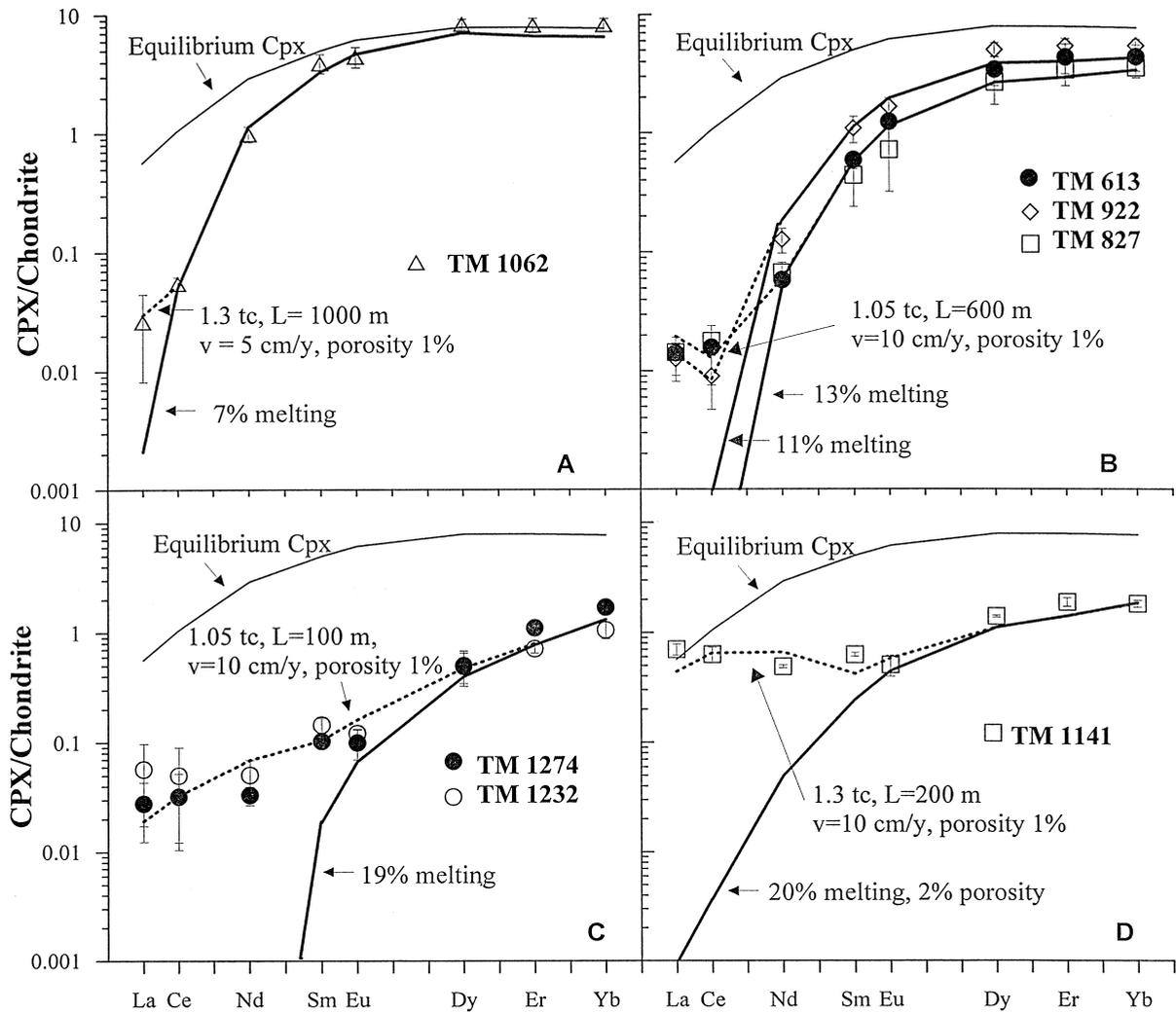
Fig. 5. (a–f). Results of modeling the peridotitic clinopyroxene compositions as partial melting followed by percolation-controlled, isomodal chromatographic exchange. Heavy lines represent the clinopyroxene concentration calculated with a critical melting model. Residual porosity during melting is 0.1% except in (d) where it is 2%. Light continuous lines are clinopyroxene (cpx) compositions in equilibrium with initial percolating N-MORB melt. Dotted lines show REE element enrichment in cpx due to chromatographic exchange of percolating melt with the modeled residue. Percolation times indicated are normalized to the time tc required to traverse the column; L is column length, v is porosity. All modeling parameters are given in Tables 2 and 3. (g) Trace element concentrations of cpx in equilibrium with: (1) reacted melt emerging from the lowermost mantle section, sample 922 (see Fig. 5b), (2) reacted melt emerging from the central mantle section (see Fig. 5c). Stippled field indicates cpx in equilibrium with binary melt mixture of 1 and 2 (mixing proportion 0.9/0.1 and 0.5/0.5 of 1 and 2, respectively). Models are compared to trace elements patterns of clinopyroxenes from transition zone rocks. Error bar corresponds to 1σ. (h) Alternative model for uppermost mantle section assuming that clinopyroxene and plagioclase are derived from an interstitial, depleted column melt as shown in line labeled 1 in Fig. 5g. Initial peridotite is virtually cpx-barren TM 1531. In order to match the composition of TM 1454, TM 1531 is mixed with 3% cpx formed in equilibrium with the column melt. For matching TM 1524, TM 1531 is mixed with 10% trapped melt which has crystallized olivine/plagioclase/cpx in proportions of 1:5:4. Following the mixing, all constituent phases are equilibrated.

the vicinity of the dunite-rich zone along the basal/central mantle section boundary (sample TM 1141). Given the additional evidence for a partial melting trend from mineral chemical data, we prefer to explain the large scale variations as a result of a partial melting history whereas small scale (<100 m) variations in the uppermost peridotites point to effects caused by reactions of the solid matrix with percolating melts.

Fractional melting and melt percolation are considered as the two processes which influenced the REE geochemistry of the peridotites. They are treated as events separated in time. Our

justification for doing so is that incompatible trace element enrichment related to a *final* melt percolation event will have the most pronounced effect on the chemistry of the peridotites. On the other hand, if such an event occurred *during* decompression melting, the melting trend (causing incompatible trace element depletion) opposes and strongly weakens percolation-related enrichment. This does not rule out that partial melting and melt migration go hand in hand but it means that the incompatible trace element record is biased towards any late event where rates of melt percolation are high compared to rates of partial melting. This likely occurs in the
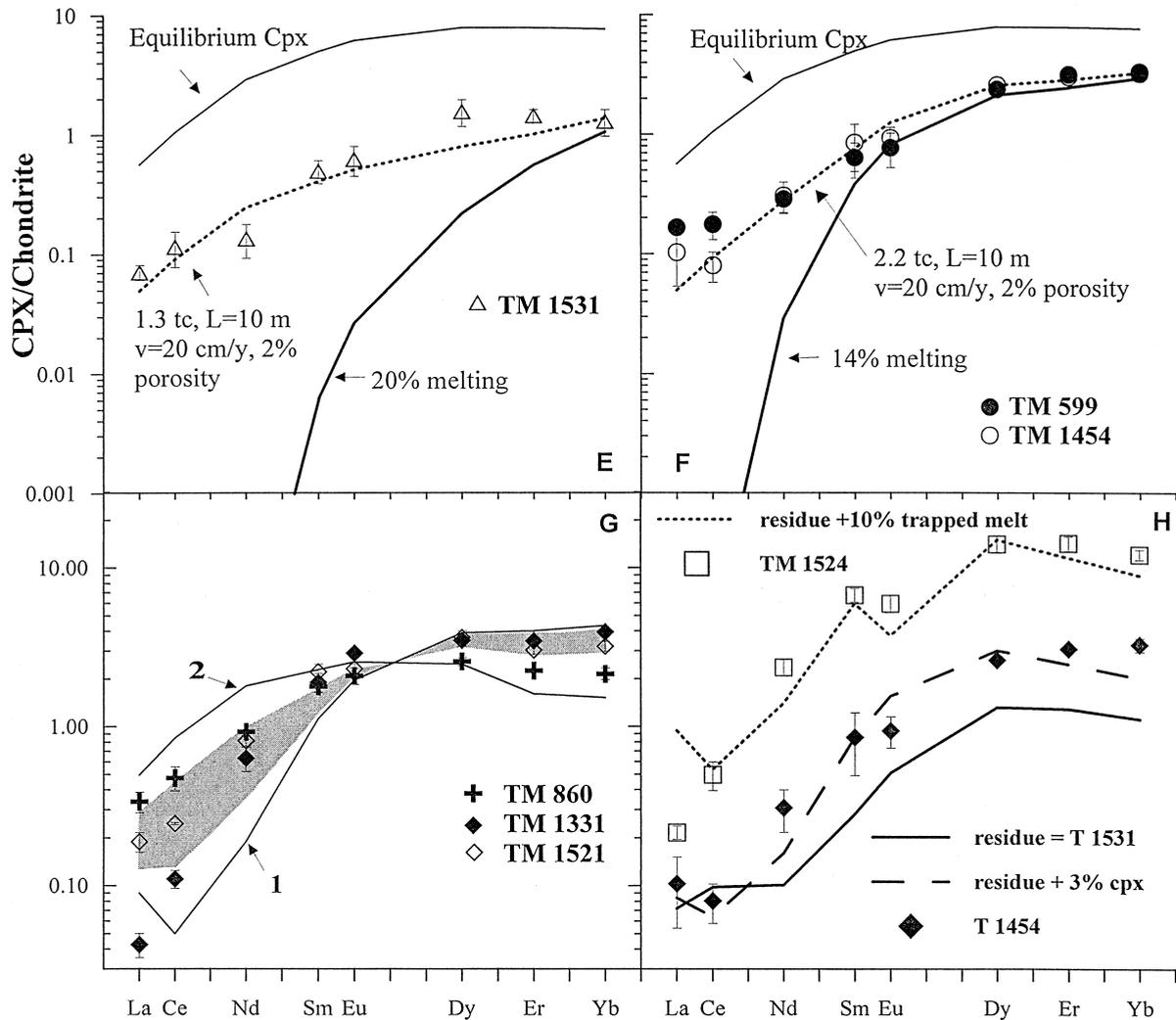
Fig. 5. (Continued)

5.2. Mantle Section

As can be seen in Fig. 5a,b, lherzolites from the lowermost mantle section closely match a residue of 7% (sample TM 1062), 11% (samples TM 613, 922, Fig. 5b), and 13% partial melting (sample TM 827, Fig. 5b) of the assumed source composition. However, La and Ce are somewhat enriched compared to the modeled residues. The patterns can be matched by using a long column length (1000–600 m) and small values of t (1.05–1.3 tc) during melt percolation. However, given that La (and Ce in TM 922) are close to the detection limit and that LREE are more prone to alteration than the other REEs, we cannot rule out at this stage that the basal peridotites are essentially free of any late stage melt percolation. The large value for the chosen grain size (Table 3) is because of the coarse porphyroclasts of orthopyroxene and cpx in the basal rocks. Currently observed matrix grain sizes of olivine and pyroxene neoblasts are much smaller, but they are thought to

postdate the melt percolation process since grain size reduction at the base of the ophiolite is attributed to detachment tectonics.

Peridotites from the central mantle section (TM 1232, TM 1274) have lower HREE concentrations than the basal peridotites, so the peridotites are thought to have formed as a residue of 19–20% melting of the assumed source (Fig. 5c). Due to the low modal cpx content, bulk D values for the peridotites are low, and the harzburgites are not significant sources or sinks for incompatible trace elements. The movement of trace element concentration fronts during melt percolation is, therefore, not significantly slowed down compared to melt velocities. A short time after the melt has reached the sample (t = tc), the required metasomatic overprint is reached (t = 1.3 to 1.05 tc, column length of 100 m, porosity 1%, 10 cm/yr velocity).

Sample TM 1141 (Fig. 5d) shows a similar degree of HREE depletion as TM 1232 and TM 1274 (i.e., similar extents of melting in our approach) but a much stronger LREE and MREE enrichment. This is accounted for in the modeling using longer times of percolation for similar column parameters (L = 200 m, porosity 1%, velocity 10 cm/yr). TM 1141 is depleted in orthopyroxene (opx, 10% modal) compared to the mode in-

ferred from the melting model (20%). This discrepancy suggests that melt migration led to modal changes such as solution of opx and precipitation of olivine with excess melt generation (Kelemen et al., 1992; Kelemen et al., 1995a,b, 1997). As shown by Godard et al. (1995), this will tend to lower the REE content of the liquid and, via concomitant olivine precipitation and diffusive exchange, also lower the solid concentrations. Whether these effects are more important than parameters used in our modeling must be tested in the future.

Peridotites from the uppermost section (TM 599, TM 1454) are modeled as products of the reaction between a residue of 14% partial melting and an N-MORB melt (Fig. 5f). In contrast to the above percolation parameters, a short column length (10 m) combined with a larger dimensionless time (t = 2.2 tc), higher porosity (2%), and higher percolation velocity (20 cm/yr) is required. Compared to the central and lower mantle section, column parameters are adjusted in such a way as to minimize fractionation among the REE. The depleted harzburgite from the same section (TM 1531) requires higher degrees of melting (20%, Fig. 5e) but can be modeled with the same column parameters.

It is notable that the extent of melting as inferred from HREEs correlates with the Cr# in the spinels (Fig. 6), commonly taken as an indicator of the degree of melting of mantle peridotite (Dick and Bullen, 1984).

The column parameters presented in this section are preferred values but are not unique. The column parameters are guided by the need of having a progressively weaker fractionation among the REEs (relative to the presumed residue from partial melting) from the lowermost to the central to the uppermost mantle section (exception T1141). This can be accomplished by choosing a shorter column length, larger porosity, or higher percolation velocity given the grain size constraints from the samples and a constant diffusion coefficient. While we have mainly varied the column length, other combinations of L, v, and porosity are acceptable. Column parameters are also dependent on the assumed composition for the percolating melt.

We have the greatest confidence in column parameters derived for the uppermost peridotites. Column length can be interpreted as distance between melt channels and the sample as long as melt *infiltration* occurs along melt channels. Dunite bands have been interpreted to reflect the location of such melt channels (Boudier and Nicolas, 1977; Kelemen et al., 1995a,b). The frequency of dunite bands in the TM massif is lowest in the basal lherzolites, high in the basal/central mantle section transition (sample T 1141), moderate in the central mantle section, and high in the uppermost section. In the latter, it is in the tens of meter range or locally shorter. Together with evidence for melt infiltration in the upper peridotites from mineral chemistry and from evidence as presented further below, this spacing of dunite bands is used to constrain the column length in the uppermost peridotites. A significant porosity in the percent range is again suggested by the abundance of melt impregnation features.

5.3. Transition Zone Rocks

Peridotites with very small amounts (TM 1521) or no opx (TM 860, TM 1331) can either represent strongly reacted residual mantle or true cumulate rocks. Their mineral compositions (i.e., c and w in Fig. 3) do not fit the melting trend defined by harzburgites and lherzolites. Assuming that the transition zone rocks represent true cumulate rocks, we evaluate if their REE pattern can be explained as cumulates formed from column-melts. The column melts are the emerging melts which were modified by reactions with the mantle matrix. The composition of the column melts was determined by the parameters which we used to model the mantle rocks of the lower and central mantle section. The only free variable was, therefore, the mixing ratio between the column melts from both mantle sections. The equilibrium cpx of the unmixed column melts are shown as thick, continuous lines marked 1 for column melts from the lower mantle (samples TM 922, TM 613) section and 2 for the central mantle section (samples TM 1232, 1274; Fig. 5g). A characteristic feature of the column melts is that, for the low melt/rock ratios implied by the modeling parameters (low porosity, long times tc but low t/tc ratios), the HREE of the melts are drastically lowered compared to the original N-MORB melt entering the column. Such low HREE concentrations also characterize the transition zone wehrlites. While there certainly are other ways to model the transition zone rocks, it is remarkable that they could represent cumulates from independently modeled column melts. Mixing ratios of column melts from the lower and central mantle sections which vary from 0.9/0.1 to 0.5/0.5 (Fig. 5g, gray shading) yield the best fit for TM 860, TM 1331, and TM 1521.

Olivine clinopyroxenite TM 7.5 represents a more evolved rock (Fo 83, Mg# of Cpx 82) and shows cpx REE patterns which are homogeneously enriched with respect to N-MORB cpx. The pattern may result from a somewhat evolved N-MORB melt.

5.4. TM 1524 and Alternative Model for Uppermost Mantle Rocks

A characteristic feature of plagioclase lherzolite TM 1524 is that the HREE content of its cpx is high (higher than one which would be in equilibrium with N-MORB) but the LREE concentration in the cpx is low (lower than cpx in equilibrium with N-MORB). Applying our approach to estimate degrees of melting in residual mantle rocks to TM 1524 implies that the residue before chromatographic reaction was an undepleted lherzolite since the HREE abundance of TM 1524 is so high. Given the isolated occurrence of this sample within depleted residual mantle rocks, the survival of such a primitive mantle lherzolite within a mantle column dominated by decompression melting is virtually impossible. Our approach to modeling this rock has, therefore, been different. It is assumed that sample 1524 has undergone a similar history as cpx-poor peridotites occurring in the immediate vicinity, i.e., TM 1531. Subsequently, however, 10% melt became trapped within this residual rock and crystallized as equal proportions of cpx and plagioclase, these values being constrained by the current modal proportions in the plagioclase lherzolite (cf. Dick, 1989). These added phases are brought into equilibrium with the existing matrix phases according to mineral/melt distribution coefficients. Using N-MORB as trapped liquid cannot reproduce the pattern of TM 1524 and a more depleted liquid is required. Evidence for such highly depleted liquids comes from the transition zone rocks modeled above. A model using the
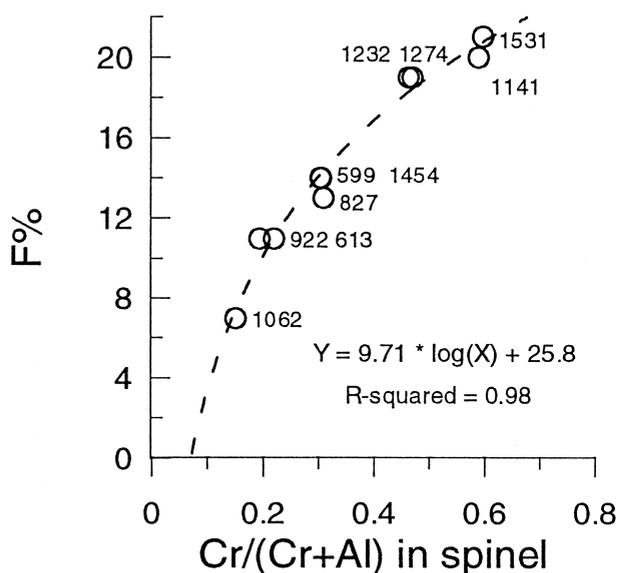
Fig. 6. Correlation between the extent of melting as determined from HREE in clinopyroxene and the Cr# of spinel for residual mantle peridotites from the Table Mountain massif.

column melt from the lowermost mantle section (given in Table 2) produces a reasonable fit (Fig. 5h).

The evidence for liquids more depleted than N-MORB suggests an alternative, geologically motivated modeling approach for the uppermost peridotites TM 599 and TM 1454. It is based on the geological and microstructural evidence that at least some of the cpx present in these samples is derived directly from a circulating melt; that is, a depleted residue was refertilized. In contrast to modeling TM 1524, the cpx from TM 599 and TM 1454 is thought to have formed by fractionation from an interstitial melt of constant composition, rather than crystallization from trapped melt. The absence of plagioclase in the peridotites supports this approach. As in TM 1524, TM 1531 is used as the initial, depleted residue which became refertilized by the addition of 3% cpx precipitating from a percolating melt (Fig. 5h). Melt-derived cpx and the initial bulk solid are equilibrated after melt removal. As in TM 1524, this model cannot reproduce the observed concentrations of TM 599 and TM 1454 as long as N-MORB is used as infiltrating melt. Using again the column melt composition from the lowermost mantle section, the pattern is better simulated. Due to the low bulk distribution coefficient of the initial host, the composition of the final cpx (after equilibration with the solid matrix) is mainly governed by the 3% cpx added and thus the melt composition present in the interstitial network (compare cpx of interstitial melt shown as line "1" in Fig. 5g with "residue + 3% cpx" in Fig. 5h).

6. DISCUSSION

The cpx REE patterns from different locations in the Table Mountain mantle section display a total variation in LREE that is only marginally greater than the variation in the HREE. For a given sample suite of mantle rocks, this feature is not uncommon on a world-wide scale (Bodinier et al., 1991; Prinzhofer and Allègre 1985; McDonough and Frey 1989; Frey et

al., 1991; van der Wal and Bodinier, 1996; Song and Frey, 1989; Takazawa et al., 1992; Downes et al., 1991). In our case, the HREE variation was modeled by near fractional melting of a uniform source. Any near fractional melting model would suggest that the LREE variation should be exceedingly high compared to that of the HREEs (see Table 2, modeled bulk rock data). The only sample which nearly matches a near fractional residue in both HREE and LREE is TM 1062. Obviously, there is a buffering mechanism which keeps the LREE concentrations of highly depleted samples from the central and upper mantle section above the current detection limits of the ion probe, at least for the samples most depleted in HREEs. As shown in the preceding section, this mechanism may well be percolation and reaction of a MORB-type melt through the peridotites. For a given set of column parameters during percolation-controlled metasomatism (i.e., a given column length, percolation velocity, porosity, grain size, diffusion coefficient) the element with the lowest bulk D in a peridotite will achieve the closest equilibration with the percolating melt. Bulk D varies also with the degree of depletion (mainly due to modal change in cpx) such that larger volumes of depleted mantle rocks will be closer to equilibrium with a percolating melt than smaller volumes of less depleted peridotite. An example using average column parameters from our study is shown in Fig. 7. The initially higher concentrations of the LREEs from the more fertile peridotite increase at such a slow rate during metasomatism that after percolation the less fertile, originally more trace element depleted sample is LREE enriched compared to the more fertile sample. It is, therefore, not surprising to find that the rocks most depleted in cpx (having the lowest bulk D) (TM 1274, TM 1232, TM 1531, TM 1141) display relatively shallow REE patterns.

Like typical abyssal peridotite (Johnson et al., 1990), the residual mantle rocks from the Table Mountain massif are not in trace element equilibrium with the volcanic carapace exposed in the Blow Me Down and North Arm Mountain massifs of the Bay of Islands Ophiolite (Suen et al., 1979; Jenner et al., 1991; Elthon, 1991). In this respect, the supra-subduction zone setting inferred for the Bay of Islands Ophiolite (Searle and Stevens, 1984; Jenner et al., 1991; Elthon, 1991; Cawood and Suhr, 1992) differs little from classic mid ocean ridges. The apparent inconsistency in the assumed source-melt relationship is resolved if the melt is considered as the accumulation of melt fractions ranging from enriched to depleted derived from the entire mantle column (e.g., Langmuir et al, 1992; Sobolev, 1996a). The presence of near fractional instantaneous melts in supra-subduction environments required by this scenario was confirmed directly by the observation of ultra-depleted melt inclusions in high-Mg olivines from the Troodos ophiolite (Cyprus) boninites and tholeiites (Sobolev, 1996b; Portnyagin et al., 1996).

Compared to the abyssal peridotite range defined by the work of Johnson et al. (1990), the Table Mountain peridotites from central and top sections tend to be more depleted. Whether this indicates a general difference between abyssal peridotites and ophiolitic (i.e., typically supra-subduction zone) mantle is difficult to say at this stage because the abyssal peridotite data base itself is biased towards fracture zones (Johnson et al., 1990), and new data from Hess Deep peridotites indicate the occurrence of very depleted mantle under ocean ridges (Dick and Natland, 1995).
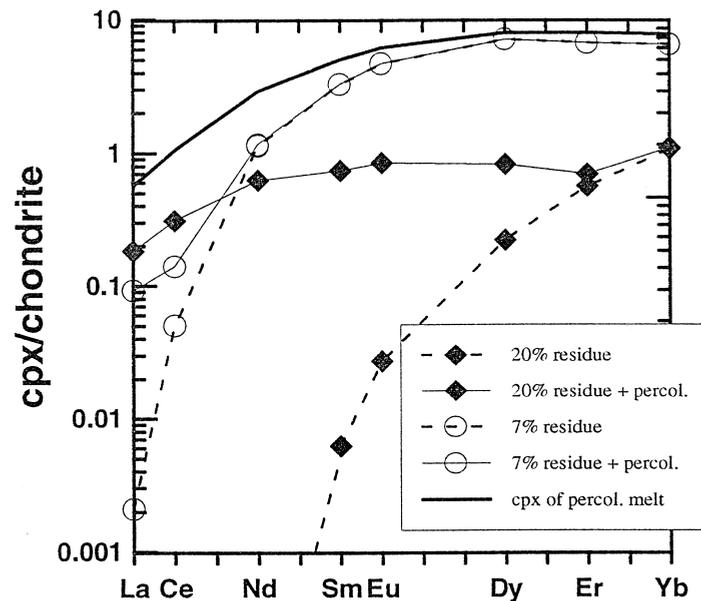
Fig. 7. Comparison of percolation controlled metasomatism affecting a residue of 7 or 20% critical melting (0.1% residual porosity). Column parameters for chromatographic exchange are grain radius 2 mm, porosity 1%, diffusion coefficient 10^{-13} cm^2/s, column length 100 m, percolation velocity 10 cm/y, infiltrating melt is N-MORB. All lines show clinopyroxene REE concentrations.

A large range in the degree of melt depletion is present in the 6 km thick mantle section of Table Mountain. This was already expected on the basis of the mineral chemistry of the mantle section (Suhr and Robinson, 1994). In the context of an upwelling mantle undergoing decompression melting, such a difference in the degree of melting for a depth range of 6 km is not well understood. In the simplest of all scenarios we can assume a triangular melting regime with a constant rate of upwelling and melt productivity. Turnover of the flow occurs at the limits of the melting regime (Plank and Langmuir, 1992). Samples whose present depth in the mantle section differ by 6 km should differ in extent of melting by only 1–2%. This value contrasts with a difference of 13% in the degree of melting observed in Table Mountains. The trend towards lower degrees of melting in the basal peridotites is regional and systematic if judged on the basis of the combination of REE data (this study) and the mineral chemistry (Suhr and Robinson, 1994). In order to explain this trend we are suggesting that the basal, less depleted lherzolite have been tectonically accreted to the ophiolite during obduction, thereby extending an accretionary concept developed for the metamorphic sole to the basal mantle section (Suhr and Batanova, submitted). The lower degrees of depletion inferred for the uppermost TM mantle rocks are less systematic than those from the base. Highly depleted samples (harzburgite TM 1531) occur within 200 m of apparently very little depleted plagioclase lherzolite TM 1524, and the apparent degrees of depletion of TM 599 and TM 1454 are intermediate. This variation might represent a mechanism of refertilization which is local and most pronounced at the crust-mantle boundary (Nicolas and Prinzhofer 1983). Possibly, then, the central and uppermost mantle sections were once depleted to a similar degree but the uppermost section became selectively refertilized. It is interesting to note that the largest chemical variability in terms of REEs in TM is present in the uppermost mantle section and that this is also the location most likely to be

sampled from the abyssal environment (Suhr and Robinson, 1994).

The nature of melts migrating through the mantle section is poorly constrained. We have used a N-MORB melt but a wide range of more enriched melts (in terms of equilibrium relative to the host peridotites) could probably be successfully used. The good correlation between the Cr# of spinel and the inferred degree of melting (Fig. 6) supports the simple model of melting followed by chromatographic exchange. In the N-MORB infiltration-model, relatively short (<500y) times of melt host reaction are inferred for the uppermost peridotites. The effectiveness of melt-host reaction in the uppermost peridotites is not due to long percolation times but due to the proximity to the feeder channels, i.e., the replenishment with unused melt.

If, on the other hand, geologic reasoning is emphasized, i.e., the evidence for melt-impregnation and the difficulty to explain the presence of less depleted peridotites in the uppermost mantle, a case can be made to suggest that a melt more depleted than N-MORB percolated through the peridotites. This evidence comes from melts in equilibrium with the transition zone rocks and from presumably impregnated samples TM 1524, TM 599, and TM 1454. Evidence for trace element exchange with depleted melts relative to N-MORB in the Bay of Islands Ophiolite has also been found in transition zone dunites from Blow Me Down Mtn. massif (Suhr et al., 1998) and in dyke rocks and lower crustal cumulates from the Lewis Hills and North Arm Mtn (for references see section Previous work). The depleted melts from TM can be modeled as column melts or mixtures of column melts but other models are viable, e.g., incomplete aggregation of fractional melts.

7. CONCLUSIONS

HREE concentrations and patterns of cpx from the Table Mountain peridotites are consistent with near fractional melting

of a depleted mantle source in the range of 7–20% of melting. A small residual porosity (0.1%) during melting is required (given the chosen distribution coefficients).

LREE concentrations and patterns of cpx from the Table Mountain peridotites are significantly higher and less fractionated than would be expected from near fractional melting scenario and show no correlation with mineral compositions.

A two stage history of the mantle peridotites is suggested: (1) formation by near-fractional melting followed by (2) interaction with a percolating aggregate melt of N-MORB or more depleted composition.

Wehrlitic rocks of the transition zone could represent cumulates which have crystallized from mixtures of melts emerging from the lowermost and central mantle sections using column parameters defined by modeling of the mantle rocks. These melts are more depleted than N-MORB. Evidence for depleted melts relative to N-MORB might also be locked into the chemistry of some of the uppermost peridotites using a melt impregnation model.

The range in the degrees of depletion observed in the mantle section is much higher than would be expected by decompression melting in simple upwelling mantle scenarios. The less depleted nature of the lowermost peridotites might be caused by tectonic accretion during obduction whereas for the less depleted uppermost peridotites, a refertilization model is a plausible explanation.

REFERENCES

Anders E. and Grevesse N. (1989) Abundance of the element: Meteoritic and Solar. *Geochim. Cosmochim. Acta* **53,** 197–214.

Bédard J. H. and Hébert R. (1996) The lower crust of the Bay of Islands Ophiolite, Canada: Petrology, mineralogy, and the importance of syntexis in magmatic differentiation in ophiolites and at ocean ridges. *J. Geophys. Res.* **101,** 25105–25124.

Bodinier J.-L., Vasseur G., Vernieres J., Dupuy C., and Fabries J. (1990) Mechanisms of mantle metasomatism: Geochemical evidence from the Lherz orogenic peridotite. *J. Petrol.* **31,** 597–628.

Bodinier J. L., Menzies M. A., and Thrill M. F. (1991) Continental to oceanic mantle transition-REE and Sr-Nd isotopic geochemistry of the Lanzo lherzolite massif. In *Orogenic Lherzolites and Mantle Processes,* (ed. M. A. Menzies, et al.); *J. Petrol. Spec. Lherzolite Iss.,* 191–210. Oxford Univ. Press.

Bodinier J. L., Merlet C., Bedini R. M., Simien F., Remaidi M., and Garrido C. J. (1996) Distribution of niobium, tantalum, and other highly incompatible trace elements in the lithospheric mantle: The spinel paradox. *Geochim. Cosmochim. Acta* **60,** 545–550.

Boudier F. and Nicolas A. (1977) Structural controls on partial melting in the Lanzo Peridotite. In *Magma Genesis* (ed. H. J. B. Dick); *Dept. Geol. Miner. Ind. Oregon* **96,** 63–78.

Casey J. F., Elthon D. L., Siroky F. X., Karson J. A., and Sullivan J. (1985) Geochemical and geological evidence bearing on the origin of the Bay of Islands and Coastal Complex ophiolites of western Newfoundland. *Tectonophysics* **116,** 1–40.

Cawood P. A. and Suhr G. (1992) Generation and obduction of ophiolites: Constraints from the Bay of Islands Complex, western Newfoundland. *Tectonics* **11,** 884–897.

Czamanske G. K., Sisson T. W., Campbell J. L., and Teesdale W. J. (1993) Micro-PIXE analysis of silicate reference standards. *Amer. Mineral.* **78,** 893–903.

Dick H. J. B. (1989) Abyssal peridotites, very slow spreading ridges and ocean ridge magmatism. In *Magmatism in the Ocean Basins.* (ed. A. D. Sounders and M. J. Norry) *Geol. Soc. Spec. Publ.* 71–105.

Dick H. J. B. and Bullen T. (1984) Chromian spinel as a petrogenetic indicator in abyssal and alpine-type peridotites and spatially associated lavas. *Contrib. Mineral. Petrol.* **86,** 54–76.

Dick H. J. B. and Natland J. H. (1995) Late stage melt evolution and transport in the shallow mantle beneath the East Pacific Rise. *Proc. Ocean Drill. Prog. Sci. Res.* **147,** 103–134.

Downes H., Bodinier J. L., Thirlwall M. F., Lorand J. P., and Fabries J. (1991) REE and Sr-Nd isotopic geochemistry of Eastern Pyrenean Peridotite Massifs: Subcontinental lithospheric mantle modified by continental magmatism. In *Orogenic lherzolites and mantle processes* (ed. M. A. Menziers et al.); *J. Petrol. Spec. Lherzolite Iss.* 97–115. Oxford Univ. Press.

Dunning G. R. and Krogh T. E. (1985) Geochronology of ophiolites of the Newfoundland Appalachians. *Canadian J. Earth Sci.* **22,** 1659–1670.

Edwards S. J. (1990) Harzburgites and refractory melts in the Lewis Hills Massif, Bay of Islands Ophiolite Complex: The base-metals and precious-metals story. *Canadian Mineral.* **28,** 537–552.

Edwards S. J. and Malpas J. (1995) Multiple origins for mantle harzburgites: Examples from the Lewis Hills, Bay of Islands ophiolite, Newfoundland. *Canadian J. Earth Sci.* **32,** 1046–1057.

Elthon D. (1991) Geochemical evidence for formation of the Bay of Islands ophiolite above a subduction zone. *Nature* **354,** 140–143.

Elthon D., Karson J. A., Casey J. F., Sullivan, J., and Siroky, F. X. (1986) Geochemistry of diabase dikes from the Lewis Hills massif, Bay of Islands ophiolite: Evidence for partial melting of oceanic crust in transform faults. *Earth Planet. Sci. Lett.* **78,** 89–103.

Forsyth D. W. (1993) Crustal thickness and the average depth and degree of melting in fractional melting models of passive flow beneath Mid-Ocean Ridges. *J. Geophys. Res.* **98,** 16073–16079.

Frey F. A., Shimizu N., Leinbach A., Obata M., and Takazawa E. (1991) Compositional variations within the Lower Layered Zone of the Horoman Peridotite, Hokkaido, Japan: Constraints on models for melt-solid segregation. In *Orogenic Lherzolite and Mantle Processes* (ed. M. A. Menzies et al.); *J. Petrol. Spec. Lherzolite Iss.,* 211–227. Oxford Univ. Press.

Godard M., Bodinier J.-L., and Vasseur G. (1995) Effects of mineralogical reactions on trace element redistributions in mantle rocks during percolation processes: A chromatographic approach. *Earth Planet. Sci. Lett.* **133,** 449–461.

Hart S. R. and Dunn T. (1993) Experimental cpx/melt partitioning of twenty-four trace elements. *Contrib. Mineral. Petrol.* **113,** 1–8.

Hauri E. H. and Hart S. R. (1994) Constraints on melt migration from mantle plumes: A trace element study of peridotite xenoliths from Savai'i, Western Samoa. *J. Geophys. Res.* **99,** 24301–24321.

Hess P. C. (1992) Phase equilibria constraints on the origin of ocean floor basalts. In *Mantle Flow and Melt Generation at Mid-Ocean Ridges* (ed I. Phipps Morgan et al.); *Geophys. Monogr.* **71,** 67–102. AGU.

Jacobsen S. B. and Wasserburg G. J. (1979) Neodymium and Strontium isotopic study of the Bay of Islands ophiolite complex and the evolution of the source of midocean ridge basalts. *J. Geophys. Res.* **84,** 7429–7445.

Jenner G. A., Dunning G. R., Malpas J., Brown M., and Brace T. (1991) Bay of Islands and Little Port Complexes, revisited: Age, geochemical, and isotopic evidence confirm supra-subduction zone origin. *Canadian J. Earth Sci.* **28,** 1635–1652.

Johnson K. T. M., Dick H. J. B. (1992) Open-system melting and temporal and spatial variation of peridotite and basalts at the Atlantis II Fracture Zone. *J. Geophys. Res.* **97,** 9219–9241.

Johnson K. T. M., Dick H. J. B., Shimizu H. (1990) Melting in the oceanic upper mantle: An ion microprobe study of diopsides in abyssal peridotites. *J. Geophys. Res.* **95,** 2661–2678.

Kelemen P. B., Dick H. J. B., and Quick J. E. (1992) Formation of harzburgite by pervasive melt/rock reaction in the upper mantle. *Nature* **358,** 635–641.

Kelemen P. B., Shimizu N., Salters V. J. M. (1995a) Extraction of mid-ocean-ridge basalt from the upwelling mantle by focused flow of melt in dunite channels. *Nature* **375,** 747–753.

Kelemen P. B., Whitehead J. A., Aharonov E., Jordahl K. A. (1995b) Experiments on flow focusing in soluble porous media, with appli-

cations to melt extraction from the mantle. *J. Geophys. Res.* **100,** 475–496.

Kelemen P. B., Hirth G., Shimizu N., Spiegelman M., and Dick H. J. B. (1997) A review of melt migration processes in the adiabatically upwelling mantle beneath oceanic spreading centers. *Phil. Trans. Roy. Soc. London A* **355,** 283–318.

Kennedy A. K., Lofgren G. E., Wasserburg G. J. (1993) An experimental study of trace element partitioning between olivine, orthopyroxene and melt in chondrules: Equilibrium values and kinetic effects. *Earth Planet. Sci. Lett.* **115,** 177–195.

Langmuir C. H., Klein E. M., and Plank T. (1992) Petrological systematics of mid-ocean ridge basalts: Constraints on melt generation beneath ocean ridges. In *Mantle Flow and Melt Generation at Mid-Ocean Ridges* (ed. J. Phipps Morgan, et al.), pp. 183–280. AGU.

Maaloe S. (1982) Geochemical aspects of permeability controlled partial melting and fractional crystallization in the mantle. *Geochim. Cosmochim, Acta* **46,** 43–57.

McDonough W. F. and Frey F. A. (1989) Rare earth elements in upper mantle rocks. In *Geochemistry and Mineralogy of Rare Earth Elements* (eds. B. R. Lipin and G. A. McKay), pp. 99–145. MSA.

McKenzie D. (1984) The generation and compaction of partially molten rock. *J. Petrol.* **25,** 713–765.

McKenzie D. and Bickle M. J. (1988) The volume and composition of melt generated by extension of the lithosphere. *J. Petrol.* **29,** 625–679.

Navon O. and Stolper E. (1987) Geochemical consequences of melt percolation: The upper mantle as a chromatographic column. *J. Geol.* **95,** 285–307.

Nicolas A. (1986) A melt extraction model based on structural studies in mantle peridotites. *J. Petrol.* **27,** 999–1022.

Nicolas A. (1989) *Structures of Ophiolites and Dynamics of Oceanic Lithosphere.* Kluwer.

Nicolas A. and Prinzhofer A. (1983) Cumulative or residual origin for the transition zone in ophiolites: Structural evidence. *J. Petrol.* **24,** 188–206.

Ozawa K. and Shimizu N. (1995) Open-system melting in the upper mantle: Constraints from the Hayachine-Miyamori, northeastern Japan. *J. Geoph. Res.* **100,** 22315–22355.

Plank T. and Langmuir C. H. (1992) Effects of the melting regime on the composition of the oceanic crust. *J. Geophys. Res.* **97,** 19747–19770.

Prinzhofer A. and Allègre C. J. (1985) Residual peridotites and the mechanisms of partial melting. *Earth Planet. Sci. Lett.* **74,** 251–265.

Portnyagin M. V., Magakyan R., and Schmincke H.-U. (1996) Geochemical variability of boninite magmas: evidence from magmatic inclusions in highly magnesian olivine from lavas of southwestern Cyprus. *Petrology* **4,** 231–246.

Rampone E., Hofmann A. W., Piccardo G. B., Vannucci R., Bottazzi P., and Ottolini L. (1996) Trace element and isotope geochemistry of depleted peridotites from an N-MORB type ophiolite (Internal Liguride, N. Italy). *Contrib. Mineral. Petrol.* **123,** 61–76.

Roden M. F. and Shimizu N. (1993) Ion microprobe analyses on the composition of the upper mantle beneath the Basin and Range and Colorado plateau provinces. *J. Geoph. Res.* **98,** 14091–14108.

Searle M. P., and Stevens R. K. (1984) Obduction processes in ancient, modern, and future ophiolites. In *Ophiolites and Oceanic Lithosphere* (ed. I. G. Gass, et al.); *Geol. Soc. Spec. Publ.* **13,** 303–315.

Shimizu N. and Hart S. R. (1982) Isotope fractionation in secondary ion mass spectrometry. *J. Appl. Phys.* **53,** 1303–1311.

Siroky F. X., Elthon D. L., and Butler J. C. (1985) Major element variations in basalts and diabases from the North Arm Mountain Massif, Bay of Islands Ophiolite: Implications for magma chamber processes at mid-ocean ridges. *Tectonophysics* **116,** 41–61.

Sleep N. H. (1988) Tapping of melt by veins and dikes. *J. Geophys. Res.* **93,** 10255–10272.

Sobolev A. V. (1996a) Inclusions in minerals as a source of principal petrologic information. *Petrology* **4,** 209–220.

Sobolev A. V. (1996b) Primary melts at mid-ocean ridges, mantle plumes, and subduction-related plate margins: Constraints on mantle melting. *J. Conf. Abstr.* **1,** 584.

Sobolev A. V. and Batanova V. G. (1995) Mantle Lherzolites of the Troodos Ophiolite complex, Cyprus: Clinopyroxene geochemistry. *Petrology* **3,** 440–448.

Sobolev A. V. and Shimizu N. (1992) Extremely depleted magmas and oceanic mantle permeability. *Dokl. Akad. Nauk* **326,** 354–360.

Sobolev A. V. and Shimizu N. (1993) Ultra-depleted primary melt included in an olivine from the mid-Atlantic Ridge. *Nature* **363,** 151–154.

Sobolev A. V., Migdisov Al-dr.A., and Portnyagin M. V. (1996) Incompatible elements partitioning between clinopyroxene and basaltic melt based on the study of melt inclusions in minerals from Troodos, Cyprus. *Petrology* **4,** 307–317.

Song Y. and Frey F. A. (1989)Geochemistry of peridotite xenoliths in basalt from Hannuoba, Eastern China: Implications for subcontinental mantle heterogeneity. *Geochim. Cosmochim. Acta* **53,** 97–113.

Suen C. J., Frey F. A., and Malpas J. (1979) Bay of Islands ophiolite suite, Newfoundland: Petrologic and geochemical characteristics with emphasis on rare earth element geochemistry. *Earth Planet. Sci. Lett.* **45,** 337–348.

Suhr G. (1992) Upper mantle peridotites in the Bay of Islands Ophiolite, Newfoundland: Formation during the final stages of a spreading center? *Tectonophysics* **206,** 31–53.

Suhr G. (1993) Evaluation of upper mantle microstructures in the Table Mountain Massif (Bay of Islands Ophiolite). *J. Struct. Geol.* **15,** 1273–1292.

Suhr G. and Batanova V. (1997) Basal lherzolite in the Bay of Islands Ophiolite: Origin by detachment-related telescoping of a ridge-parallel melting gradient. *Terra Nova* (submitted).

Suhr G. and Robinson P. T. (1994) Origin of mineral chemical stratification in the mantle section of the Table Mountain Massif (Bay of Islands Ophiolite). *Lithos* **31,** 81–102.

Suhr G., Seck H. A., Shimizu N., Günther D., and Jenner G. (1998) Circulation of refractory melts in the lowermost oceanic crust: Evidence from a trace element study of dunite- and gabbro-hosted clinopyroxenes in the Bay of Islands Ophiolite. *Contrib. Mineral. Petrol.* (in press).

Sun S-S., and McDonough W. F. (1989) Chemical and isotopic systematics of oceanic basalts: Implications for mantle composition and processes. In *Magmatism in the Ocean Basins* (ed. A. D. Saunders and M. J. Norry) *Geol. Soc. Spec. Publ.,* 313–345.

Takazawa E., Frey F. A., Shimizu N., Obata M., and Bodinier J. L. (1992) Geochemical evidence for melt migration and reaction in the upper mantle. *Nature* **359,** 55–58.

van der Wal D. and Bodinier J. L. (1996) Origin of the recrystallization from the Ronda peridotite by km-scale pervasive porous melt flow. *Contrib. Mineral. Petrol.* **122,** 387–405.

Varfalvy V., Hébert R., Bédard J. H., and Laflèche M. R. (1997) Petrology and geochemistry of pyroxenite dykes in upper mantle peridotites of the North Arm Mountain Massif, Bay of Islands Ophiolite, Newfoundland: Implications for the genesis of boninitic and related magmas. *Canadian Mineral.* **35,** 543–570.

Vasseur G., Vernieres J., and Bodinier J.-L. (1991) Modeling of trace element transfer between mantle melt and heterogranular peridotite matrix. *J. Petrol.* **32,** 41–54.

Williams H. (1979) Appalachian Orogen in Canada. *Canadian J. Earth Sci.* **16,** 792–807.